IET Research Journals

Submission Template for IET Research Journal Papers

IET Journals
The Institution of Engineering and Technology

Enhanced Predictor-Corrector Mars Entry Guidance Approach with Atmospheric Uncertainties

ISSN 1751-8644
doi: 0000000000
www.ietdl.org

Xu Jianwei[1], *Qiao Jianzhong*[1,2], *Guo Lei*[1,2*], *Chen Wenhua*[1,3]

[1] *School of Automation Science and Electrical Engineering, Beihang University, No. 37, Xueyuan Road, Haidian District, Beijing, China*
[2] *Beijing Advanced Innovation Center for Big Data-based Precision Medicine, Beihang University, No. 37, Xueyuan Road, Haidian District, Beijing, China*
[3] *Department of Aeronautical and Automotive Engineering, Loughborough University, Loughborough, LE11 3TU, U.K.*
* *E-mail: lguo@buaa.edu.cn*

Abstract: Due to the long-range data communication and complex Mars environment, the Mars lander needs to promote the ability to autonomously adapt uncertain situations ensuring high precision landing in future Mars missions. Based on the analysis of multiple disturbances, this paper demonstrates an enhanced predictor-corrector guidance method to deal with the effect of atmospheric uncertainties during the entry phase of the Mars landing. In the proposed method, the predictor-corrector guidance algorithm is designed to autonomously drive the Mars lander to the parachute deployment. Meanwhile, the disturbance observer is designed to onboard estimate the effect of fiercely varying atmospheric uncertainties resulting from rapidly height decreasing. Then, with the estimation of atmospheric uncertainties compensated in the feed-forward channel, the composite guidance method is put forward such that both anti-disturbance and autonomous performance of the Mars lander guidance system are improved. Convergence of the proposed composite method is analyzed. Simulations for a Mars lander entry guidance system demonstrates that the proposed method outperforms the baseline method in consideration of the atmospheric uncertainties.

Nomenclature

g_0	=	gravitational acceleration at R_0, approximately 3.7 m/s^2
L, D	=	nondimensional aerodynamic lift and drag acceleration, g
R_0	=	radius of the Mars, 3,397,200 m
r	=	radial distance from the Mars$'$ center to the vehicle, normalized by R_0
s	=	great-circle range to go, normalized by R_0
V	=	Mars-relative velocity, normalized by $\sqrt{g_0 R_0}$
γ	=	Mars-relative flight-path angle, deg
ρ	=	atmospheric density of Mars, kg/m^3
σ	=	bank angle, deg
C_L, C_D	=	coefficient of lift and drag force, $-$
τ	=	time, normalized by $\sqrt{R_0/g_0}$

1 Introduction

Since guided entry guidance is firstly adopted in the latest Mars landing mission, the 2011 Mars Science Laboratory (MSL), and successfully achieved a higher landing precision than ever before [1], Mars lander entry guidance algorithms have become a hot research topic [2-4]. Nevertheless, further improvement of guidance precision is inevitably limited by many unpredictable aspects, such as initial state deviation, atmospheric uncertainty and inertial measurement unit inaccuracy [1],[5]. On the other hand, autonomous guidance ability is required such that Mars landers can survive long period mission without real-time data communication. Therefore, both anti-disturbance and autonomous performance of Mars landers are needed to be addressed to satisfy the high guidance precision demand of future Mars landing missions.

Generally speaking, guidance methods could be mainly separated into two categories: 1) reference-path tracking schemes [6-9], and 2) predictive path-planning schemes [3],[10-17]. The idea of reference trajectory tracking is first introduced into the entry guidance in the 1970s with the fundamental purpose of cancelling the tracking errors between the reference and the actual path [6]. By comparing to the reference-path tracking method, the predictive approach could provide greater flexibility for landers to handle larger initial states dispersions and accommodate more severe off-nominal conditions. Besides, the predictive methodology can alleviate the burden on actuators which resolves the overload problem on tracking pre-programmed trajectory under poor maneuverability. In [10], the predictor-corrector technique has been first attempted to guide a Mars lander to ensure the satisfaction of the mission requirements. Besides, [11] uses predictive path-planning schemes to plan a path onboard from the current position to the targeting parachute deployment. Moreover, the numerical predictor-corrector algorithm is used to deliver the spacecraft to satisfy certain conditions [12]. Specifically, Lu successfully extends the predictor-corrector technique to various types of spacecrafts and provides a general guidance design structure [13]. In order to reduce the large onboard computational time of integration, segmented guidance is designed in [3] to improve the online performance of the predictor-corrector algorithm.

Although the predictive guidance scheme holds greater potential to be adaptive and flexible than the reference-path tracking guidance, it relies heavily on accurate onboard models of the vehicle [14]. Until now, some effective approaches have been provided to achieve satisfiable performance on solving constant biases in uncertainties [13],[15]. However, the Martian environment contains large uncertainties resulting from the limited observational atmospheric data and the rapidly changing atmosphere dynamics on Mars, it brings a significant adverse impact on the accuracy of the existing technique. Therefore, atmospheric uncertainties should be online mitigated more radically than it is usually done by repetitive control corrections [11],[15-17].

Recently, the investigation of systems subject to uncertainties and disturbances has received considerable research attention and many effective control methods are proposed [18-30]. In [18], Lam comprehensively analyzes the estimation problem of reachable set and extends the algorithm to the situation with parameter uncertainties. In order to deal with a class of parametric uncertain systems with

both sensor and actuator saturations, elegant disturbance attenuation approach is proposed to achieve the prescribed performance [19]. While as a typical disturbance rejection approach, disturbance observer based control (DOBC) method has achieved notable performance [22-25]. Guo proposes hierarchical anti-disturbance control (CHADC) strategy by combining DOBC with traditional control methods, such as H_∞ control, backstepping control, sliding mode control, finite-time control, composite control with prescribed performance, et al [26-32]. Besides simple structure and flexible design, the most significant advantage of CHADC comparing with the other anti-disturbance methods is that it holds the performance of simultaneous disturbance compensation and attenuation by taking the partial attainable information into account.

Motivated by the above observations, we consider the Mars entry guidance with atmospheric uncertainties. In this paper, the main contributions can be summarized as following:

1. As compared to the previous researching work, multiple sources of disturbances are considered and analyzed to find the main disturbance before the design of guidance scheme;
2. Different from the fading-memory filter technique dealing with constant bias atmospheric uncertainties, disturbance observer is designed in this paper to estimate the height-dependent bias atmospheric uncertainties; and
3. The composite guidance approach based on the DOBC is proposed to conquer the effect of the atmospheric uncertainties such that the desired parachute deployment precision can be guaranteed.

The remaining part of the paper is organized as follows: Section 2 provides the multiple disturbances models and analysis; in Section 3 the disturbance observer based predictor-corrector guidance scheme is introduced; simulation results are demonstrated in Section 4 to testify the effectiveness of the proposed algorithm, followed by the conclusion in Section 5.

2 Multiple Disturbances Models and Analysis

In this paper, a longitudinal dimensionless model [4] is considered. As the Mars lander entries the atmosphere of Mars with a relatively high speed and low height compared with the rotational speed of Mars, the Mars$'$ rotational effects are ignored. Therefore, the kinematic and dynamic equations of an Mars lander during the atmosphere entry phase are given by

$$\dot{r} = V\sin\gamma + \bar{d}_1 \tag{1}$$

$$\dot{V} = -D - \left(\frac{\sin\gamma}{r^2}\right) + \bar{d}_2 \tag{2}$$

$$\dot{\gamma} = \frac{L}{V}\left[\cos\sigma + \left(V^2 - \frac{1}{r}\right)\left(\frac{\cos\gamma}{rL}\right) + \bar{d}_3\right] \tag{3}$$

$$L = \frac{1}{2}\rho(1+\Delta\beta)V^2\frac{S}{m}(C_L + \Delta C_L) \tag{4}$$

$$D = \frac{1}{2}\rho(1+\Delta\beta)V^2\frac{S}{m}(C_D + \Delta C_D) \tag{5}$$

where m is the mass of Mars lander, S represents the Mars lander reference area. $\bar{d}_1$ represents the wind disturbance, $\bar{d}_2$ represents equivalent disturbance brought by drag coefficients uncertainties and atmospheric uncertainties, $\bar{d}_3$ represents equivalent disturbance brought by lift coefficients uncertainties and atmospheric uncertainties [5],[33-34].

Generally, the disturbances will cause different degrees of effect according to certain missions. In order to compare the impact degree of multiple disturbances and find main disturbance to deal with, Monte Carlo simulations have been made to demonstrate the parachute deployment dispersions under different disturbances. The engineering applied guidance method Apollo guidance is adopted in the simulations [7]. The simulation parameters and uncertainties configurations are shown in Table 1 referring to Jet Propulsion Laboratory and NASA researchers [5].

It needs to be noted that the atmospheric perturbation $\Delta\beta$ which is a variable with zero mean and standard deviation σ_β. σ_β can be modeled as a function of height r and topographic surface height z_s by the relation [33-34]

$$\sigma_\beta = 0.01(25 + z_s)\exp[(r - R_0 - 100)/40] \tag{6}$$

Each Monte Carlo simulation runs 1000 cases and simulation results are shown in Figs. 1(a)-1(e).

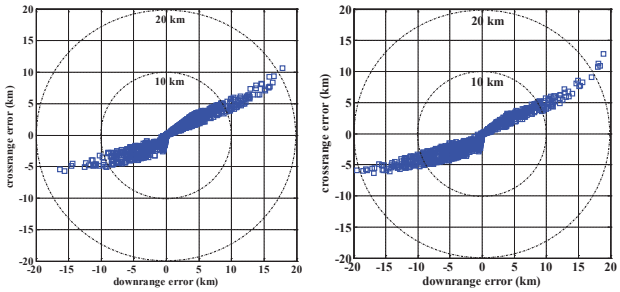

(a) Deployment Dispersions under Atmospheric Uncertainties in Eq. (6)

(b) Deployment Dispersions under Atmospheric Uncertainties with $\Delta\beta = 0.15$

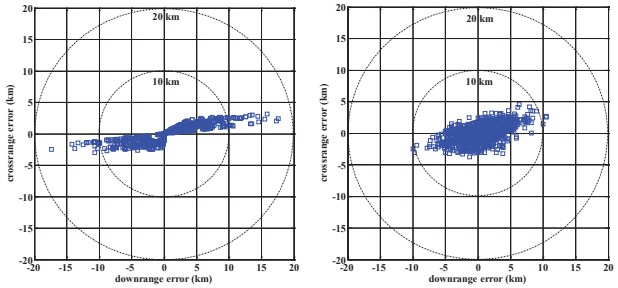

(c) Deployment Dispersions under Initial State Deviation

(d) Deployment Dispersions under Dynamic Parameter Uncertainties

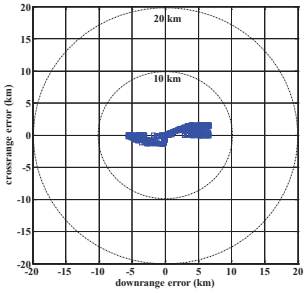

(e) Deployment Dispersions under Wind Uncertainties

Fig. 1: Deployment Dispersions under Multiple Sources of Uncertainties

Remark 1: As can be seen from Figs. 1(a)-1(e), the effect of the atmospheric uncertainties is mostly noticeable in downrange out of the initial state deviation, dynamic parameter uncertainties and wind uncertainties. It needs to be noticed from Fig. 1(a) and (b), the dispersion is lager Thus, the purpose of the paper is to achieve a higher precision of the parachute deployment by attenuating the atmospheric uncertainties among multiple disturbances. In the following paragraph, the influence of the atmospheric uncertainties is mainly focused. Dealing with multiple and mismatched disturbances will be studied in the next work.

Aiming at tackling with the disturbance caused by the atmospheric uncertainty in the control channel, the Mars entry guidance system Eqs. (1)-(5) are simplified as follows

$$\dot{r} = V\sin\gamma \tag{7}$$

Table 1 Monte Carlo campaign parameters

Disturbances	Initial state deviation			Wind		Coefficients uncertainties	
Parameters	r_0, km	$V_0, m/s$	γ_0, deg	$>60\ km, m/s$	$<60\ km, m/s$	C_L	C_D
Value	125	5505	-14.15	0	0	0.41	1.71
Perturbations	$\Delta r, km$	$\Delta V, m/s$	$\Delta\gamma, deg$	–	–	ΔC_L	ΔC_D
Range (3σ)	± 2.31	± 2.85	$\pm 15\%$	± 80	± 40	$\pm 15\%$	$\pm 15\%$

$$\dot{V} = -D - \left(\frac{\sin\gamma}{r^2}\right) \tag{8}$$

$$\dot{\gamma} = \frac{L}{V}\left[\cos\sigma + \left(V^2 - \frac{1}{r}\right)\left(\frac{\cos\gamma}{rL}\right) + d_3\right] \tag{9}$$

$$L = \frac{1}{2}\rho(1+\Delta\beta)V^2\frac{S}{m}C_L \tag{10}$$

$$D = \frac{1}{2}\rho(1+\Delta\beta)V^2\frac{S}{m}C_D \tag{11}$$

$d_3 = \Delta\beta\cos\sigma$. According to Eq. (6), $\Delta\beta$ falls into $(-3\sigma, 3\sigma)$ with the probability of 99.74%. Subsequently, for the simplicity of analysis, $\Delta\beta$ is considered to be upper bounded by 3σ in the following paragraph. It should be noted that the disturbance effect also exists in the mismatched velocity channel which is not directly dealt by the proposed method in this paper.

3 Disturbance Observer Based Predictor-Corrector Control

In this section, the disturbance observer based predictor-corrector approach is designed to deal with the system constructed by Eqs. (7)-(11). The proposed composite anti-disturbance controller structure is illustrated in Fig. 2. The proposed controller consists of nominal predictor-corrector method ensuring the Mars lander flying to the parachute deployment and disturbance observer estimating atmospheric uncertainties simultaneously. Following the predictor-corrector method is introduced first, the disturbance observer based composite controller is then designed.

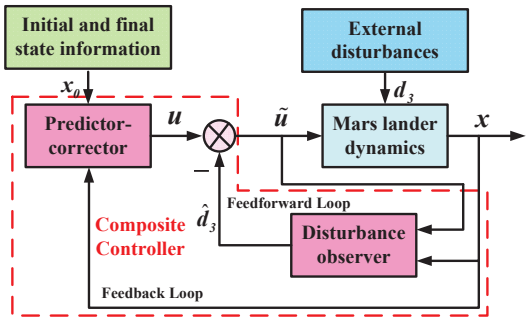

Fig. 2: The Composite Controller Structure

3.1 Predictor-Corrector Algorithm

Up to date, the predictor-corrector guidance algorithm [10] is successfully applied in the entry mission of spacecrafts due to its advantage of high autonomy and precision. Therefore, in order to utilize the predictor-corrector guidance scheme in the Mars entry mission, some variables are firstly defined. Taking s to represent the range to go along the Mars surface linking the current location of Mars lander to the parachute deployment site. Thus, one can get

$$\dot{s} = -\frac{V\cos\gamma}{r} \tag{12}$$

The differentiations are with respect to the dimensionless time τ (normalized by $\sqrt{R_0/g_0}$). As time is not the crucial criteria during the entry phase, the time variable is substituted for an energy variable E containing altitude and velocity providing for the criterions of parachute deployment:

$$E = \frac{1}{r} - \frac{V^2}{2} \tag{13}$$

From Eq. (13), E is a monotonically increasing variable ($dE/d\tau = DV > 0$). Because V can be determined by the values E and r, three longitudinal equations are given as follows

$$\frac{ds}{dE} = -\frac{\cos\gamma}{rD} \tag{14}$$

$$\frac{dr}{dE} = \frac{\sin\gamma}{D} \tag{15}$$

$$\frac{d\gamma}{dE} = \frac{L}{DV^2}\left[\cos\sigma + \left(V^2 - \frac{1}{r}\right)\left(\frac{\cos\gamma}{rL}\right) + d_3\right] \tag{16}$$

Given initial conditions $s(E_0)$, $r(E_0)$ and $V(E_0)$, the lander has to meet the final constraint $s_f = s(E_f)$ when the energy E comes to the specific final value $E_f = 1/{r_f}^* - {V_f}^{*2}/2$ (${r_f}^*$ and ${V_f}^*$ represent the height and velocity of the parachute deployment). It should be pointed out that since the Mars atmospheric density is too thin for the lander to execute effective command during the initial phase of the flight, the predictor-corrector algorithm is called only when the lift force can provide a sufficient component to drive the lander. Thus, $\lambda = \sqrt{L^2 + D^2}$ is defined to give an index calling algorithm when λ achieves a certain level to provide enough lifting capability; if not, the bank angle command is set to be zero.

The bank angle magnitude profile is parameterized by a linear function of E:

$${\sigma_0}^{(k+1)} = {\sigma_0}^{(k)} - \lambda_k \frac{z({\sigma_0}^{(k)})}{\left[z({\sigma_0}^{(k)}) - z({\sigma_0}^{(k-1)})\right]}\left({\sigma_0}^{(k)} - {\sigma_0}^{(k-1)}\right) \tag{17}$$

where

$$z(\sigma_0) = s(E_f) - {s_f}^* = 0 \tag{18}$$

the step-size parameter λ_k is chosen to be $1/2^i$ and i is the smallest integer (including 0) such that $f({\sigma_0}^{(k+1)}) < f({\sigma_0}^{(k)})$ with the stopping condition

$$\left|\frac{\partial f({\sigma_0}^{(k+1)})}{\partial\sigma_0}\right| = \left|z({\sigma_0}^{(k+1)})\frac{\partial z({\sigma_0}^{(k+1)})}{\partial\sigma_0}\right| \le \varepsilon \tag{19}$$

Remark 2: It needs to be noticed that the predictor-corrector guidance scheme calculation can only use the information about nominal models. However, from Eq. (16) one can see that the disturbance d_3 causes effect to γ, this will further affects range s. As a result, to overcome the effect of disturbance d_3 in the command calculation is a core problem to be figured out.

3.2 Disturbance Observer

For a system such as a Mars lander, precisely modeling its dynamics and directly measuring the disturbances onboard are very difficult because of the dramatic uncertainty of the atmosphere. Fortunately, fading-memory filter technique is applied to solve the uncertainties

problem and achieves satisfiable performance [12-13],[15-16]. Nevertheless, constant effects of uncertainties are focused in above literatures. Alternatively, the disturbance observer technique provides an approach which can deal with more general kinds of disturbances [35]. In this subsection, a nonlinear disturbance observer is designed to estimate the uncertainties in the models. $d_3' = Ld_3/V$ is defined and Eq. (9) can be rewritten as

$$\dot{\gamma} = \frac{L}{V}\cos\sigma + \left(V^2 - \frac{1}{r}\right)\left(\frac{\cos\gamma}{Vr}\right) + d_3' \tag{20}$$

Then the following disturbance observer is given to estimate the effect of disturbance d_3'

$$\dot{z} = -l\left(\frac{L}{V}\cos\sigma + \left(V^2 - \frac{1}{r}\right)\frac{\cos\gamma}{Vr}\right) - l\left(z + l\gamma\right) \tag{21}$$

$$\hat{d}_3' = z + l\gamma \tag{22}$$

where z is the internal state variable of the observer, l is the observer gain. It can be derived that $\hat{d}_3 = \hat{d}_3' V/L$. By defining the estimate error between the disturbance and the disturbance estimation as $e_{d_3'} = d_3' - \hat{d}_3'$, the performance of the disturbance observer is analyzed as follows.

Combining Eqs. (7)-(11) together with Eqs. (21)-(22) gives

$$\begin{aligned}
\dot{e}_{d_3'} =& \dot{d}_3' - \dot{\hat{d}}_3' = \dot{d}_3' - \dot{z} - l\dot{\gamma} \\
=& l\left(\frac{L}{V}\cos\sigma + \left(V^2 - \frac{1}{r}\right)\frac{\cos\gamma}{rV}\right) + l\left(z + l\gamma\right) \\
& - \frac{l}{V}\left[L\cos\sigma + \left(V^2 - \frac{1}{r}\right)\left(\frac{\cos\gamma}{r}\right)\right] - ld_3' + \dot{d}_3' \\
=& lz + l^2\gamma - ld_3' + \dot{d}_3' \\
=& -le_{d_3'} + \dot{d}_3'
\end{aligned}$$

Then one can get

$$e_{d_3'} = \dot{d}_3'/l + \left(e_{d_3'}(t_0) - \dot{d}_3'/l\right)\exp\left(-l(t - t_0)\right) \tag{23}$$

Taking the description of d_3 and system Eqs. (7)-(11) into account, one will have

$$\dot{d}_3' = \frac{\partial \dot{d}_3'}{\partial \Delta\beta}\frac{\partial \Delta\beta}{\partial t} + \frac{\partial \dot{d}_3'}{\partial \cos\sigma}\frac{\partial \cos\sigma}{\partial t} \tag{24}$$

where $\dot{d}_3' = f(V, r, \gamma)$ is derived which is assumed to be bounded by $0 < \mu < \infty$. Then by introducing Eq. (23), it is possible to ensure that as $t \to \infty$, if $l > 0$ is chosen, the estimation error will enter into the set $\left|e_{d_3'}\right| \leq \mu/l$. It can be seen that the bound of disturbance estimation error can be made arbitrarily small, comparing with the disturbance d_3, as l increases. Consequently, e_d will also converge to a upper bounded domain as V and L are positive.

Remark 3: It can be seen from Eq. (24) that the boundary of $\dot{d}_3'$ is decided by the derivative of $\Delta\beta$ and $\cos\sigma$. The derivative of $\cos\sigma$ is inherently bounded. Then, during the entry phase of Mars landing, the varying of atmosphere is related to the density of atmosphere which varies continuously along with the height. Therefore, d_3' is bounded by μ is reasonable.

3.3 The Composite Controller

Uncertainties in the Mars atmosphere may significantly degrade the entry performance of lander. With the disturbance estimated by the disturbance observer, the predictor-corrector method can take into account of the disturbance by replacing it with its estimated value which achieves the desired parachute deployment performance. With the definition of $u = \cos\sigma$ the structure of the composite controller is given in

$$\tilde{u} = u - \hat{d}_3 \tag{25}$$

Substitute the composite guidance scheme Eq. (25) into system Eq. (9), one can derive that

$$\dot{\gamma} = \frac{L}{V}\left[\cos\sigma + \left(V^2 - \frac{1}{r}\right)\left(\frac{\cos\gamma}{rL}\right) + e_{d_3}\right] \tag{26}$$

According to the analysis in the preceding part, the estimation error e_{d_3} will converge into a bounded set with the predictor-corrector guidance scheme attenuating the estimation error. Thus, the effect of the disturbance d_3 is ultimately dealt by the proposed composite guidance scheme.

Remark 4: The disturbance observer based predictor-corrector composite guidance scheme Eq. (25) consists of two layers: the inner layer contains the disturbance observer and the compensator in the feedforward path which is operated through disturbance estimation $\hat{d}_3$; the outer layer contains the predictor-corrector controller onboard which calculates the bank angle command to satisfy the requirements in feedback path which is operated through u and the bank angle command follows Eq. (17). Therefore, the composite hierarchical structure proposed in this paper could simultaneously guarantee the anti-disturbance ability and the guidance precision of Mars landers.

4 Numerical Simulations

The lander model adopted in the simulations is the model from Mars Science Laboratory. The geometry of the lander is a double-cone, with an aero-shell forebody shape of a 70 deg sphere-cone. By offsetting the center of gravity from the lander axis, the lander adopts an asymmetrical orientation with respect to the incoming flow which provides a small amount of lift. The trim angle of attack is $\alpha = -15$ deg. Comparing with the landers previously, the Mars Science Laboratory has the capability of changing the flying trajectory, although the L/D is just 0.24. It also has a large volume of which the diameter is 4.5 m. The maximum bank rate of the vehicle is limited at 20 deg/s and the maximum bank acceleration at 5 deg/s^2. The simulation is based on the parameters given in Table 2. The uncertainty is selected following the distribution as Eq. 6. The observer gain $l = 0.4$ is chosen. Considering the lifting capability of the lander, λ is set at 1.52 m/s^2 [5].

From Figs. 3-6 one can see that when the altitude and the velocity of the lander satisfy the conditions of the parachute deployment, the final range of the proposed composite method is 0.005 km which is reasonable to apply to the Mars entry mission. We can first conclude that the proposed approach can guarantee the lander achieving the desired control performance under the nominal conditions.

Remark 5: The parachute deployment basically requires landers to satisfy velocity and height requirement. Then the final range is the main evaluation index in the longitudinal motion analysis.

Then for the purpose of investigating the effect of atmospheric uncertainties to the performance, several cases of the uncertainty in Eqs. (9)-(11) is chosen. $\Delta\beta$ in each case is selected according to Eq. (6) and 1 out of 1000 simulation cases is demonstrated as follows.

Table 2 The lander entry and final conditions

Parameters	Symbols	Values
initial height	r_0	125 km
initial velocity	V_0	5505 m/s
initial range	s_0	744 km
initial flight-path angle	γ_0	-14.15 deg
final height	${r_f}^*$	10 km
final velocity	${V_f}^*$	410 m/s
final range	${s_f}^*$	37 km
final flight-path angle	γ^*	-

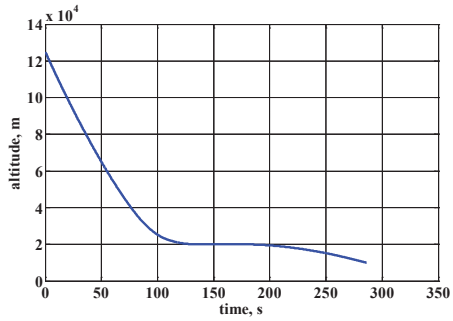

Fig. 3: Altitude History

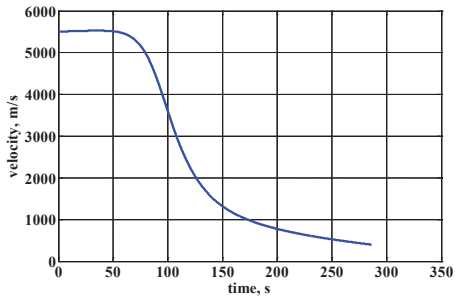

Fig. 4: Velocity History

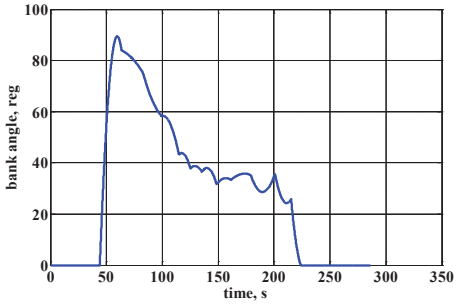

Fig. 5: Bank Angle History

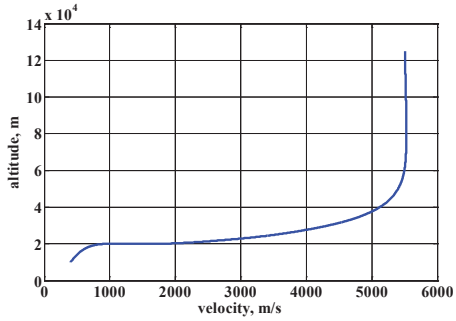

Fig. 6: Altitude-Velocity History

Table 3 The final range precision of the lander in the entry phase

	Nominal case	Atmospheric Uncertainties as Eq. (6)
Baseline algorithm	0.005 km	6.153 km
Predictor-corrector+DO	0.005 km	1.216 km

From blue curves in Figs. 7 and 8, one can see that when the lander reaches the parachute deployment altitude, uncertainties

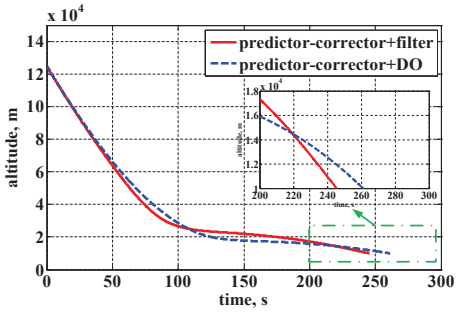

Fig. 7: Altitude History and Magnified History

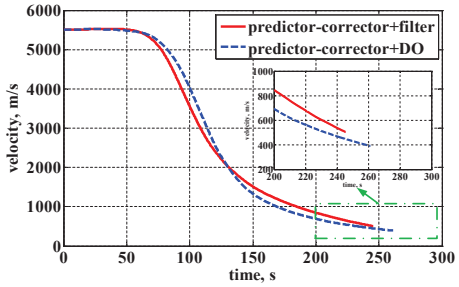

Fig. 8: Velocity History and Magnified History

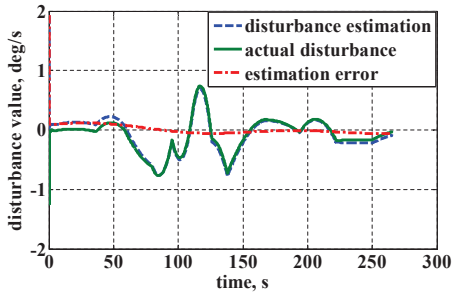

Fig. 9: Disturbance History and Estimation of Disturbance

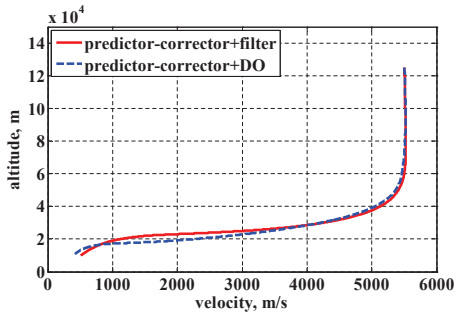

Fig. 10: Altitude-Velocity History

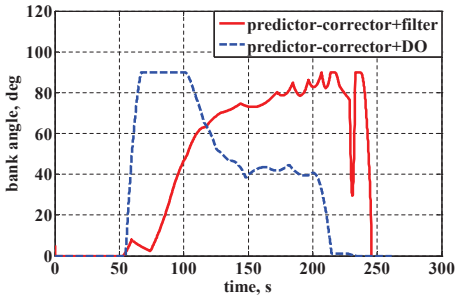

Fig. 11: Bank Angle History

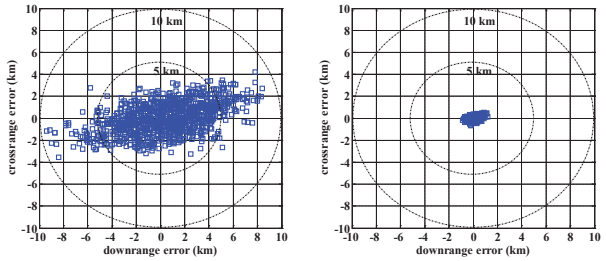

a) Deployment Dispersions under Baseline Algorithm

b) Deployment Dispersions under Composite Controller

Fig. 12: Deployment Dispersions under Atmospheric Uncertainties Only with uncertainties in Eq. (6)

in atmosphere cause the lander operated under baseline algorithm (predictor-corrector+filter) to have a larger velocity and cost more fuel. The lander need to fly a longer distance to satisfy the final parachute deployment requirement. For a lander flying during the entry phase, final range is crucial to evaluate the precision of the parachute deployment. The final parachute deployment precision using different methods is shown in Table 3. Results show that the final range is 6.153 km when using the predictor-corrector method which is not suitable for the high-precision requirement of parachute deployment. However, comparing to the baseline method, Figs. 7 and 8 demonstrate that the proposed method can successfully restrain the effect of atmospheric uncertainties and make the lander more likely flying under no disturbance circumstances. Fig. 9 also demonstrates that the disturbance observer is efficient to estimate the disturbance which varies complicatedly. Thus, the proposed composite method can improve the accuracy of the parachute deployment. On the other hand, one can see that the inconstant varying disturbance degrades the performance achieved by the baseline control. The final range of the composite guidance method is 1.216 km which is a more sophisticated entry guidance strategy than that of the baseline approach. The performance of 1000 cases illustrated in Fig. 12 indicates that the composite guidance scheme achieves a better mission precision than that of baseline guidance strategy in the existence of atmospheric disturbance.

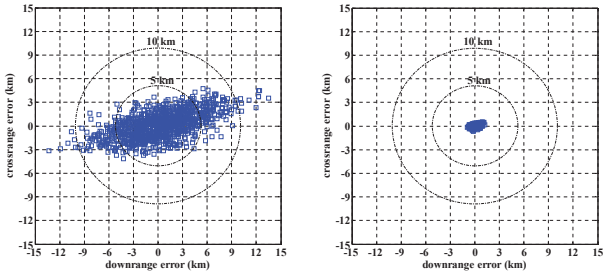

a) Deployment Dispersions under Baseline Algorithm

b) Deployment Dispersions under Composite Controller

Fig. 13: Deployment Dispersions under Multiple Disturbances

In order to evaluate the disturbances attenuating ability and reliability performance of the proposed composite method under multiple disturbances, the final parachute deployment dispersions are also exhibited in 1000 runs Monte Carlo simulations for the comparison of algorithms. The uncertainty parameters and perturbations adopted in the simulations are listed in Table 1. As can be seen from Fig. 13, parachute deployment error of nearly all cases of the proposed composite method are within 2 km and that of 80.6% cases of the baseline algorithm are within 5 km. Hence, it can be seen that the proposed composite guidance approach achieves a better overall performance.

5 Conclusions and Future Work

In this paper, the novel enhanced guidance approach has been put forward to achieve high precision requirement during the entry phase of Mars landing. The approach is constructed with the predictor-corrector algorithm and the disturbance observer. The predictor-corrector algorithm is designed without depending on the scanty prestored data such that the Mars lander autonomy is well improved. On the other hand, the disturbance observer is designed to estimate the effect of atmospheric uncertainties which are compensated in the feedforward channel. Then, by using the estimation provided by the nonlinear dynamic disturbance observer, the enhanced guidance method is proposed. The Monte Carlo simulation results have verified that the proposed composite method not only reduces the effect of main disturbance during the entry process but also achieves favourable performance with consideration of multiple disturbances. It should be noted that, the real-time proposed method will cause calculation burden which may degrade the performance of guidance system in a great extent. Therefore, research on releasing the calculation burden of real-time approach will be carried out.

6 Acknowledgments

The author(s) disclosed receipt of the following financial support for the research, authorship, and/or publication of this article: This work was supported by the National Natural Science Foundation of China (grant numbers 61627810, 61320106010, 61633003, 61661136007 and 61603021), the Program for Changjiang Scholars and Innovative Research Team (grant number IRT_16R03) and Innovative Research Team of National Natural Science Foundation of China (grant number 61421063).

7 Conflict of Interest

We declare that we have no financial and personal relationships with other people or organizations that can inappropriately influence our work, there is no professional or other personal interest of any nature or kind in any product, service and/or company that could be constructed as influencing the position presented in, or the review of, the manuscript entitled.

8 References

[1] Mendeck, G.F., Craig, L.E.: 'Entry guidance for the 2011 Mars Science Laboratory mission', AIAA Atmospheric Flight Mechanics Conference, Portland, Oregon, 2011, AIAA Paper 2011-6639

[2] Dai, J., Xia, Y.: 'Mars atmospheric entry guidance for reference trajectory tracking', Aerosp. Sci. Technol., 2015, 45, pp. 335-345

[3] Xia, Y., Shen, G., Zhou, L., et al.: 'Mars entry guidance based on segmented guidance predictor-corrector algorithm', Control Eng. Pract., 2015, 45, pp.79-85

[4] Furfaro, R., Wibben, D.R.: 'Mars atmospheric entry guidance via multiple sliding surface guidance for reference trajectory tracking', AIAA/AAS Astrodynamics Specialist Conference, Minneapolis, Minnesota, 2012, AIAA Paper 2012-4435

[5] Knocke, P.C., Wawrzyniak, G.G., Kennedy, B.M.: 'Mars Exploration Rovers landing dispersion analysis', AIAA/AAS Astrodynamics Specialist Conference and Exhibit, Providence, Rhode Island, 2013, AIAA Paper 2004-5093

[6] Harpold, J.C., Graves, C.A.: 'Shuttle Entry Guidance', J. Astronautical Sci., 1979, 37, (3), pp. 239-268

[7] Carman, G.L., Ives, D.G., Geller, D.K.: 'Apollo-derived Mars precision landing guidance', AIAA Atmospheric Flight Mechanics Conference, 1998, AIAA Paper 98-4570

[8] Talole, S.E., Benito, J., Mease, K.D.: 'Sliding mode observer for drag tracking in entry guidance', AIAA Guidance, Navigation and Control Conference and Exhibit, Hilton Head, South Carolina, 2007, AIAA Paper 2007-6851

[9] Liu, Y., Pu, Z., Yi, J.: 'Observer-based robust adaptive T2 fuzzy tracking control for flexible air-breathing hypersonic vehicles', IET Control Theory Appl., 2018, 12, (8), pp. 1036-1045

[10] Powell, R.W.: 'Numerical roll reversal predictor-corrector aerocapture and precision landing guidance algorithm for Mars Surveyor Program 2001 missions', AIAA Atmospheric Flight Mechanics Conference, 1998, AIAA Paper 1998-4574

[11] Lu, P.: 'Predictor-corrector entry guidance for low-lifting vehicles', J. Guid. Control Dyn., 2008, 31, (4), pp. 1067-1075

[12] Brunner, C.W., Lu, P.: 'Skip entry trajectory planning and guidance', J. Guid. Control Dyn., 2008, 31, (5), pp.1210-1219

[13] Lu, P.: 'Entry guidance: a unified method', J. Guid. Control Dyn., 2014, 37, (3), pp. 713-728

[14] Kluever, C.A.: 'Entry guidance performance for Mars precision landing', J. Guid. Control Dyn., 2008, 31, pp. 1537-1544

[15] Brunner, C., Lu, P.: 'Comparison of fully numerical predictor-corrector and Apollo skip entry guidance algorithms', J. Astronautical Sci., 2012, 59, (3), pp. 517-540
[16] Lu, P., Cerimele, C., Tigges, M., et al.: 'Optimal aerocapture guidance', J. Guid. Control Dyn., 2015, 38, (4), pp. 553-565
[17] Kozynchenko, A.I.: 'Analysis of predictive entry guidance for a Mars lander under high model uncertainties', Act Astronaut., 2011, 68, pp. 121-132
[18] Wang, Z., Ho, D., Dong, H., et al.: 'Robust H-infinity finite-horizon control for a class of stochastic nonlinear time-varying systems subject to sensor and actuator saturations', IEEE Trans. Autom. Control, 2010, 55, (7), pp. 1716-1722
[19] Li, S., Jiang, X.: 'RBF neural network based second-order sliding mode guidance for Mars entry under uncertainties', Aerosp. Sci. Technol., 2015, 43, pp. 226-235
[20] Lam, J., Zhang, B., Chen, Y., et al.: 'Reachable set estimation for discrete-time linear systems with time delays', Int. J. Robust Nonliear Control, 2015, 25, (2), pp. 269-281
[21] Yuan, Y., Yuan, H., Wang, Z., et al.: 'Optimal control for networked control systems with disturbances: a delta operator approach', IET Control Theory Appl., 2017, 11, (9), pp. 1325-1332
[22] Zerar, M., Cazaurang, F., Zolghadri, A.: 'Coupled linear parameter varying and flatness-based approach for space re-entry vehicles guidance', IET Control Theory Appl., 2009, 3, (8), pp. 1081-1092
[23] Sun, H., Hou, L., Zong, G., et al.: 'Composite anti-disturbance attitude and vibration control for flexible spacecraft', IET Control Theory Appl., 2017, 11, (14), pp. 2383-2390
[24] Wei, Y., Zheng, W., Xu, S.,: 'Anti-disturbance control for nonlinear systems subject to input saturation via disturbance observer', Syst. Control Lett., 2015, 85, pp. 61-69
[25] Chen, W.: 'Nonlinear disturbance observer enhanced dynamic inversion control of missiles', J. Guid. Control Dyn., 2003, 26, pp. 161-166
[26] You, M., Zong, Q., Tian, B., et al.: 'Comprehensive design of uniform robust exact disturbance observer and fixed-time controller for reusable launch vehicles', IET Control Theory Appl., 2018, 12, (5), pp. 638-648
[27] Guo, L., Chen, W.: 'Disturbance attenuation and rejection for systems with nonlinearity via DOBC approach', Int. J. of Robust Nonlinear Control, 2005, 15, pp. 109-125
[28] Wei, X., Guo, L.: 'Composite disturbance observer based control and Hinf control for complex continuous models', Int. J. Robust Nonlinear Control, 2010, 20, pp. 106-118
[29] Guo, L., Cao, S.: 'Anti-disturbance control for systems with multiple disturbances', (CRC Press, 2013)
[30] Sun, H., Guo, L.: 'Neural network-based DOBC for a class of nonlinear systems with unmatched disturbances', IEEE Trans. Neural Netw. Learn. Syst., 2017, 28, pp. 482–489
[31] Qiao, J., Zhang, D., Zhu, Y., et al.: 'Disturbance observer-based finite-time attitude maneuver control for micro satellite under actuator deviation fault', Aerosp. Sci. Technol., 2018, 82-83, pp. 262–271
[32] Zhu, Y., Qiao, J., Guo, L.: 'Adaptive sliding mode disturbance observer-based composite control with prescribed performance of space manipulators for target capturing', IEEE Trans. Ind. Electron., 2019, 66, (3), pp. 1973–1983
[33] Justus, C.G., James, B.F., Johnson, D.L.: 'Mars Global Reference Atmospheric Model (Mars-GRAM 3.34): programmer's guide', Technical Report, NASA Marshall Space Flight Center Huntsville, AL, United States, 1996
[34] Justus, C.G., James, B.F., Bougher, S.W., et al.: 'Mars-GRAM 2000: a Mars Atmospheric Model for engineering applications', Adv. Space Res., 2002, 29, (2), pp. 193-202
[35] Guo, L., Cao, S.: 'Anti-disturbance control theory for systems with multiple disturbances: a survey', ISA Trans., 2014, 53, (4), pp. 846-849